SEISMIC BASE SHEAR MODIFICATION FACTORS FOR TIMBER-STEEL HYBRID STRUCTURE: A COLLAPSE RISK ASSESSMENT APPROACH

M.A. Bezabeh[1], S. Tesfamariam, M.ASCE[2‡], M. Popovski[3], K. Goda[4] and S.F. Stiemer[5]

Abstract:

In this paper, to supplement the *National Building Code of Canada*, over-strength and ductility-related force modification factors are developed and validated using a collapse risk assessment approach for a timber-steel hybrid structure. The hybrid structure incorporates Cross Laminated Timber (CLT) infill walls within steel moment resisting frames. Following the FEMA P695 procedure, initially, archetype buildings of 3-, 6-, and 9-storey height with middle bay infilled with CLT were developed. Subsequently, a nonlinear static pushover analysis is performed to quantify the actual over-strength factors of the hybrid archetype buildings. To check the FEMA P695 acceptable collapse probabilities and Adjusted Collapse Margin Ratios (ACMRs), Incremental Dynamic Analysis is carried out using 60 ground motion records that are selected to regional seismic hazard characteristics in southwestern British Columbia, Canada. Considering the total system uncertainty, comparison of the calculated ACMRs with the FEMA P695 requirement indicates the acceptability of the proposed over-strength and ductility factors.

Keywords: Wood-hybrid system; CLT infill walls; Force modification factors; Incremental dynamic analysis; Adjusted collapse margin ratio

---

[1] PhD student, School of Engineering, University of British Columbia, 3333 University Way, Kelowna, BC, Canada, V1V 1V7, Tel: (250)-808-3864, E-mail: matiyas.bezabeh@alumni.ubc.ca

[2] Associate Professor, School of Engineering, University of British Columbia, 3333 University Way, Kelowna, BC, Canada, V1V 1V7, Tel: (250)-807-8185, E-mail: Solomon.Tesfamariam@ubc.ca; ‡*Corresponding author*

[3] Principal Scientist, FPInnovations, and Adjunct Professor, University of BC, 2665 East Mall, Vancouver, BC, Canada, V6T 1W5, Tel: (604)-222-5739, E-mail: marjan.popovski@fpinnovations.ca

[4] Senior Lecture, Department of Civil Engineering, University of Bristol, United Kingdom; Queen's Building, University Walk, Bristol, United Kingdom, BS8 1TR, Tel: 0117-33-15516; E-mail: katsu.goda@bristol.ac.uk

[5] Emeritus Professor, Dept. of Civil Engineering, The University of British Columbia, Vancouver Campus, 6250 Applied Science Lane, Vancouver, B.C., Canada, V6T 1Z4, Tel: (604) 822-6301; E-mail: sigi@civil.ubc.ca

INTRODUCTION

The recent worldwide surge in research to enhance the sustainability of the current urban-form draws the attention of construction stakeholders towards the use of timber buildings. In Canada, the 2015 edition of the National Building Code (NBC) has raised the height limits for wood-frame buildings from four to six storeys. Recently, new design provisions for Cross Laminated Timber (CLT) have been included in the 2016 to supplement the 2014 CSAO86, the Canadian Standard for Engineering Design in Wood. While wood-frame construction is limited to six storeys, some innovative CLT-hybrid systems can use the alternative solution path available in the Codes, and can go to greater heights. To this end, several mid- and high-rise CLT-based buildings are constructed in Europe, North America, and Australia (Fragiacomo and van de Lindt 2016; Pie et al. 2014). To increase the applicability of CLT constructions located in moderate- and high-seismic risk, several experimental and numerical researches have been recently conducted (Poh'sié et al. 2015; Popovski and Garvic 2015; Yasamura et al. 2015; Ceccotti et al. 2013; Gagnon and Pirvu 2011; Popovski et al. 2010). For CLT system and mass-timber hybrid building, Pie et al. (2013) and Zhang et al. (2015) have developed seismic force reductions factors, respectively.

Recently, a novel steel-timber hybrid building system was developed and investigated at The University of British Columbia and FPInnovations (Dickof 2013, Stiemer et al. 2012a, b). The hybrid structure contains CLT-infill walls in steel moment resisting frames (SMRFs) as shown in Figure 1. This hybrid system is achieved by L-shaped steel connection brackets and aimed at combining light-weight and stiff CLT panels with ductile and strong SMRFs. The seismic capacity and structural efficiency of these types of connections have been reported elsewhere (Schneider et al. 2014; Pozza et al. 2014; Flatscher et al. 2014; Rinaldin et al. 2013; Fragiacomo et al. 2011).

Earlier studies on this hybrid structure considered CLT infill walls as non-structural elements (Dickof et al. 2014, Dickof 2013). Tesfamariam et al. (2014) showed the significance of CLT infill walls on seismic capacity of steel moment frame structures, and suggested the implication of considering the panels as a structural element. In Canada, for seismic design of structures, the NBC allows the use of an Equivalent Static Force Procedure (ESFP) design method with appropriate overstrength factor R_o and ductility factor R_d. However, the R_o and R_d factors for the proposed hybrid structure are not available in the NBC (NRC 2010). Dickof et al. (2014) developed preliminary values of R_o and R_d factors using static pushover analysis and did not consider the collapse risk. Bezabeh et al. (2015) developed performance-based design approach for this hybrid structure. In this paper, following FEMA's Quantification of Building Seismic Performance Factors document (FEMA P695, 2009), the R_o and R_d factors are developed.

BASE SHEAR MODIFICATION FACTORS QUANTIFICATION FRAMEWORK

FEMA's Quantification of Building Seismic Performance Factors document (FEMA P695, 2009) has been followed for the development of base shear modification factors of the hybrid structure under consideration. FEMA's quantification process is based on probabilistic collapse risk assessment of selected archetype buildings. This procedure comprises selection and development of archetype buildings, accurate nonlinear modeling, representative ground motion record selection and scaling, advanced static and dynamic analysis, and collapse risk assessment. In each of these analysis steps, uncertainties in ground motions, design, modeling, and testing are explicitly considered. However, in this paper, certain modifications were made in the FEMA P695 procedure to suit the NBC design practice and Vancouver's seismic hazard conditions. The modifications were: (1) the R factor that is investigated in FEMA P695 (2009) and that is used in the US (ASCE7-15) was substituted by an equivalent ductility related factor (R_d) and overstrength related factor (R_o), as per NBC, and (2) probabilistic seismic hazard assessment and deaggregation was carried out for the City of Vancouver, BC considering the contributions from crustal (shallow), sub-crustal (deep), and subduction earthquakes. Figure 2 shows the framework to quantify the base shear modification factors.

ARCHETYPE DEVELOPMENT AND DESIGN

The archetype buildings were selected based on the FEMA P695 guideline. Regular in the plan, *index archetype buildings* were selected based on previous studies (Bezabeh 2014 and Bezabeh et al. 2015). The selection was aimed at assessing different building heights and fundamental periods that represent the typical application of these hybrid buildings. Therefore, 3-, 6-, and 9-storey middle bay infilled hybrid structures were considered representing low-, mid-, and high-rise hybrid buildings, respectively. Initial preliminary optimization analysis showed the middle bay infilled hybrid buildings with 800 mm bracket spacing has acceptable seismic performance in terms of maximum and residual deformation responses. The bay widths considered were: 9 m for the exterior bay and 6 m for the interior bay (Figure 3). The first storey height was 4.5 m and the height of all other storeys above was 3.65 m. A bracket spacing of 800 mm and three layers of CLT panel (99 mm thickness) were considered. Panel crushing strength was equal to 11.5 MPa.

Seismic design category dictates special design and detailing requirements, and subsequently influences inelastic deformation capacity at component level. As a result, steel design category of Limited Ductility (LD) of the NBC 2010 (NRC 2010) was used during the design process. All the index archetype buildings were designed and detailed as perimeter frames with seismic to gravity weight of 4. Each building was designed using the ESP by considering a live load of 4.8 kPa for typical office floors and a load of 2.4 kPa elsewhere. Dead loads were considered for floors and roofs as 4.05 kPa and 3.4 kPa, respectively, according to the NBC 2010. The buildings studied were assumed to be located in Vancouver, BC, Canada on class C soil condition (dense soil and soft rock). The steel members designed were assumed to have properties of common hot-rolled steel, such as yield strength F_y of 350 MPa and modulus of elasticity E_s of 200 GPa. As per the FEMA P695 requirement, initially base shear modification factors were assumed as R_d = 4 and R_o = 1.5 based on initial seismic performance and iterative design checks. An equivalent static load calculation method from the NBC 2010 was adopted to distribute the design base shear along the height of the building. Tables 1 and 2, respectively, summarize the design details of the beam and column sections for the hybrid buildings.

NONLINEAR STRUCTURAL MODELING OF ARCHETYPE BUILDINGS

To perform nonlinear static and dynamic analysis of the developed archetype buildings, accurate and representative nonlinear numerical models are needed. For this purpose, numerical modeling was carried out using the Open System for Earthquake Engineering Simulation (OpenSees) finite element program (Mazzoni et al. 2006). Figure 4 shows the modeling and calibration process. The procedure outlined in Figure 4 entails:

- Carrying out component level experimental tests
- Numerical modeling of bracket connection and CLT wall
- Calibrating the numerical models of components using the experimental data
- Assembling the components to form the hybrid system

Component level testing, modeling, and calibration

Modeling of steel frame members, spread inelasticity principle

The steel frame members were modelled with nonlinear *displacement-based beam-column elements* and *linear-elastic beam-column elements*. The nonlinear beam-column elements were used at the end of the member (to represent the spreading plastic hinge zone) as displayed in Figure 4, and linear beam-column elements were for the middle portion of each member. This modeling approach reduces the computational time without compromising the quality of simulation outputs. Three Gauss integration points were considered to model the spread of plasticity in nonlinear elements. The nonlinear parts of steel elements use the *modified-Ibarra-Krawinkler-Deterioration model* (Lignos and Krawinkler 2010) with a *bilinear* material property. The backbone parameters of this material property, with appropriate plastic hinge length, were calculated based on the moment-curvature relationships of ASCE 41-06 (ASCE 2007).

Modeling of CLT panels

A CLT panel is a light-weight and strong pre-engineered wood product. Typically, CLT is made by gluing and pressing lumber boards in sandwich form (alternate direction) to form a stable rectangular shaped panel. For various connections and configurations, Popovski et al. (2010) performed extensive amount of testing on CLT walls (Figure 4). Based on their experimental observations and results, in this paper, CLT panels were simplified and numerically modeled as 2D linear-elastic, homogenous, and isotropic single 99 mm panel using *shell-elements* as shown in Figure 4. As the behaviour of the panels in the in-plane direction is of interest, the formulation of *shell-elements* were simplified to *FourNodeQuad-elements*. The *ndMaterial-ElasticIsotropic* of OpenSees was used as a material model for these elements based on the values given in Table 3. As the deformation and nonlinearity of CLT panels are localized on the connections, the adopted modeling approaches are deemed as reasonable and accurate (Shen et al. 2013, Rinalidin et al. 2013).

Modeling of connection between CLT panels and steel frames

The connection between the steel frames and CLT walls was achieved by L-shaped steel brackets; which are bolted to the steel frames and nailed to the CLT panels. A Zero-length *two-node link nonlinear spring* element was used to represent the behaviour of the bracket that connects CLT with steel frame as shown in Figure 4. A *Pinching4-uniaxial material* model was used to represent the axial and shear behavior of these elements. Moreover, since this element has zero length, P-Δ effects along the local axis were neglected. It was also assumed that these elements do not contribute to the Rayleigh damping during the nonlinear stage of loading. Shen et al. (2013) showed a more realistic characterization of the CLT to frame connection with a *Pinching4-uniaxial material* model. Therefore, by considering the experimental data of Schneider et al. (2014) as benchmark (Figure 5), calibration of *Pinching4-uniaxial material* was carried out on SIMPSON Strong-Tie connector (90×48×3.0×16) with 18 screws (5×90mm). The cyclic loading analyses were conducted by using the CUREE loading protocol that consists of primary and trailing cycles. Numerical calibration was carried out in both axial and shear directions. The numerical results and experimental data are compared in Figures 5 (a and b) for tests along axial (parallel to the grain) and shear (longitudinal to the grain) loading directions, respectively. Figure 5 shows better agreement in the initial loading stiffness. However, the failure displacement of the experiment was shown to be larger than the numerical model prediction.

System level modeling (Assembly)

Following the component level experimental tests and numerical modeling, a typical CLT infilled SMRF system was developed. This hybrid system combines ductile steel frames with CLT walls using angular L-shaped steel bracket connections. At the interface of the wall and frame, a gap was provided in order to allow the brackets to deform and dissipate energy during lateral loading. The behaviour of the bracket and the confinement (due to axial contact between the frame and panel) were combined to form the axial component of the *two-node link element*. The confinement behaviour to account for the space between the frame and panel was modeled using the *elastic-perfectly-plastic-gap uniaxial material* (EPPG). The EPPG is a trilinear hysteretic uniaxial material model which consists of a physical gap with zero stiffness and strength, linear elastic region, and post-yielding plastic region. For the current case, the compression only gap model was considered to represent the confinement property. Since wood crushing is a local phenomenon around the steel brackets, the stress at which the material reaches a plastic state was calculated by considering the wood strength in parallel and perpendicular directions over a 200mm contact length. In order to account for densification of wood after initial fracture, the post-yield stiffness of the panel was assigned to be 1% of the elastic panel stiffness. The *EPPG gap material* and the *two-node link element* of bracket connection were combined using the parallel material combination approach as shown in Figure 6. In this approach, strains are kept equal while the stresses are added up to form a single unidirectional material model.

GROUND MOTIONS

The ground motion records selected for the FEMA P695 guideline may not be applicable to southwestern BC directly for several reasons. The regional seismicity in southwestern BC is contributed by not only shallow crustal earthquakes, but also mega-thrust Cascadia interface events and deep intraplate events (Atkinson and Goda 2011). The dominant frequency content and duration for these earthquakes are significantly different from those for the FEMA P695 far-field record set containing 22 records from worldwide shallow crustal earthquakes. In this study, the record selection was conducted based on a multiple conditional mean spectra (CMS) method (Goda and Atkinson 2011).

The method takes into account multiple target spectra representing distinct response spectral features of different earthquake types (i.e. crustal versus interface versus intraplate) and their relative contributions to overall seismic hazard. It utilizes uniform hazard spectrum and seismic deaggregation scenarios that are available from probabilistic seismic hazard analysis at a site of interest. Figure 7 (a) compares the uniform hazard spectrum at the return period (T_R) of 2500 years for Vancouver with three CMS for crustal, interface, and intraplate earthquakes for the anchor vibration period of 0.8 s, showing different spectral shapes for these events. It is noteworthy that in the FEMA P695 approach, the effect of using ground motion records with different features is taken into account through the spectral shape factor. On the other hand, the multiple CMS approach accounts for this effect more explicitly and rigorously.

The record database is an extended dataset of real mainshock-aftershock sequences by combing the PEER-NGA database (Goda and Taylor 2012) with the updated version of the Japanese earthquake database (Goda et al. 2015). The number of available mainshock-aftershock sequences is 606; among them, there are 197 crustal earthquakes, 340 interface earthquakes, and 69 intraplate earthquakes. The interface events are from the 2003 Tokachi-oki earthquake or the 2011 Tohoku earthquake (which have similar event characteristics as the expected Cascadia subduction earthquake). In this study, mainshock records of the developed database are considered.

Using the target CMS (Figure 7 (a)), a set of ground motion records was selected by comparing response spectra of candidate mainshock records with the target spectra. The total number of selected records is set to 30 (two horizontal components per record; in total, 60 record components). For instance, for the 3-storey hybrid structure, 11, 10, and 9 records are selected for the crustal, interface, and intraplate earthquakes, respectively. Because the relative contributions of the Cascadia subduction events increase with the anchor vibration period, larger-magnitude records are selected more frequently for the 9-storey structure. In the CMS-based method, response spectral matching is conducted in a least squares sense by considering the geometric mean of the response spectra of two horizontal components. For the 3-storey structure, Figures 7 (b, c, d) show the response spectra of the selected records with the target CMS for crustal, interface, and intraplate events. The detailed results for the other cases can be found in Tesfamariam et al. (2015).

NONLINEAR STATIC AND DYNAMIC ANALYSES

The OpenSees (Mazzoni et al. 2006) was used to perform both static and dynamic analyses. The presence of infill walls, steel bracket connections, and distributed plasticity elements in steel frames makes nonlinear analysis of these hybrid structures computationally intensive (Bezabeh 2014). To overcome this issue, a high-performance, task-parallel approach was implemented on 200 clusters of computers at the UBC research computing service centre.

NONLINEAR STATIC ANALYSIS

In order to quantify the actual overstrength factors of the archetype hybrid buildings, static lateral loads with an inverted triangular shape were used to push the structure until either model instability or formation of enough plastic hinges to create a sway mode of collapse. The capacity (pushover) curves are given in Figures 8 (a, c, e) for the 3-, 6-, and 9- middle bay infilled archetype hybrid buildings, respectively. Moreover, Figures 8 (b, d, f) depict the height-wise distribution of maximum interstorey drift (MISD) of the buildings at yield, maximum strength, and collapse points. It can be inferred from the figure that the maximum collapse MISD values decrease as the height of the building increases. A storey-level localized collapse mechanism is observed for the 3-storey hybrid building. Moreover, the normalized drift at yielding is found to be independent of the height of the hybrid buildings. Subsequently, the collapse MISD values of Figure 8 were used to define collapse and scale the ground motion records for Incremental Dynamic Analysis (IDA).

An equivalent energy elastic-plastic (EEEP) approximation curve (blue line on Figure 8 (a)) according to ASTM 2126-09 (2009) was used to calculate the system yielding point.

Mitchel et al. (2003) explicitly defined the overstrength-related factor as an aggregated effects due to size (R_{size}), differences between nominal and factored resistances (R_{ϕ}), difference between the actual yield strength and minimum specified yield strength (R_{yield}), due to strain hardening (R_{sh}), and additional strength before collapse mechanism (R_{mech}). In this study, due to the complexity of computing the above overstrength components for the hybrid structural elements and connections, the aggregated overstrength factor (R_o) is implicitly computed using Equation 1, as the ratio of maximum shear strength of the EEEP approximation curve ($V_{max,EEEP}$) to the design base shear (V_{design}).

$$R_o = \frac{V_{max,EEEP}}{V_{design}} \tag{1}$$

The R_o factors computed for the 3-, 6-, and 9- storey archetype hybrid buildings are 3.54, 2.81, and 2.46, respectively. Considering practical design approaches, however, the NBC 2010 (NRC 2010) sets an upper bound limit of R_o at 1.7.

INCREMENTAL DYNAMIC ANAYLSIS

To verify the acceptability of the presumed R_d factor, FEMA P695 (2009) recommends the use of partial IDA (Vamvatsikos and Cornell 2002) to calculate the median collapse capacity $\hat{S}_{CT}$ and collapse margin ratio (CMR).

$$CMR = \frac{\hat{S}_{CT}}{S_{MT}} \tag{2}$$

where S_{MT} = spectral acceleration value from the 2% in 50 years hazard spectrum at the fundamental period of the archetype structure.

In IDA, each ground motion is scaled up until sway mode collapse is achieved. Typically, IDA curves are defined using an intensity measure (IM) and corresponding engineering demand parameter (EDP). In this paper, 5% damped spectral acceleration at the fundamental period $S_T(T_1)$ and MISD are considered as IM and EDP, respectively. The median collapse intensity ($\hat{S}_{CT}$) is evaluated using the IDA results. A conservative collapse criteria was used to define the dynamic sway mode collapse of buildings. Structural hardening was only considered for MISD values less than 10% and the spectral acceleration value corresponding to the dynamic instability was considered as a collapse limit state point. The IDA results are plotted in Figure 9. In Figures 9 (a, c, e), each line represents the time history response of the building under single ground motion record. The points on each line show the MISD value corresponding to the intensity level of the ground motion.

COLLAPSE FRAGILITY CURVES

To relate the scaled spectral acceleration values with the probability of collapse, collapse fragility curves are developed from the IDA analysis results. Collapse fragility curves represent the collapse probability of the hybrid buildings when subjected to scaled ground motion records. These curves are cumulative distribution functions (CDF) that were developed by fitting a lognormal distribution through collapse data points. Figures 8 (b, d, f) show the lognormal probability distribution and collapse fragility curves for the 3-, 6-, and 9-strorey hybrid buildings. According to FEMA P695, the CMR from IDA, calculated using Equation 2, should be modified to adjusted collapse margin ratio (ACMR) to account spectral shape effects and uncertainties. The spectral shape effects and uncertainties can be accounted for by evaluating the spectral shape factor and total collapse uncertainty (β_{TOT}), respectively.

In this paper, however, the effect of spectral shapes was taken into account by selecting unique ground motion records for each archetype building. Therefore, numerically AMCR and CMR are equivalent. The average ACMR within each performance group and ACMR of individual archetype buildings will be compared to the FEMA's pre-determined acceptable ACMR values.

In FEMA P695 (2009), the total collapse uncertainty (β_{TOT}) is defined as a function of other uncertainty sources, such as record-to-record (β_{RTR}), design requirement (β_{DR}), modeling (β_{MDL}), and test data (β_{TD}). Because of its insignificant effect on the final ACMR value, FEMA P695 fixes β_{RTR} to 0.4 for structures with significant period of elongation. Even though, the period based ductility for the 9-storey hybrid building is 2.42; it is still conservative to assume β_{RTR} as 0.4. Based on FEMA P695, the design requirement uncertainty is selected as fair (β_{DR} = 0.35). For this selection the confidence in the bases of design requirement was considered as medium. Moreover, considering CLT as a new construction material and the complexity in characterizing the structural behaviour of wood, the completeness and robustness in the design method for this hybrid building was tagged as medium. Since the experimental tests on this hybrid structure are limited to its component level, the uncertainty related to test data was selected as fair (β_{TD} = 0.35). In the near future, the authors intend to perform full and reduced scale shaking table experimental tests on the hybrid structure. The uncertainty related to modeling was selected as fair (β_{MDL} = 0.35). Finally, based on these selected values, the total uncertainty was calculated using Equation 3 to be 0.726 (β_{TOT} ~ 0.75). It should be noted that the above four variables are assumed statically independent.

$$\beta_{TOT} = \sqrt{\beta_{RTR}^2 + \beta_{DR}^2 + \beta_{TD}^2 + \beta_{MDL}^2} \tag{3}$$

The increase in uncertainty from record-to-record to the total collapse uncertainty (0.75) changes the shape of the collapse fragility curves. In Figure 10, two curves are shown to illustrate the influence of uncertainty on the collapse fragility curves. The collapse fragility curve with the red line was developed by the actual obtained lognormal standard deviation of collapse data points, and the curve in blue is the "adjusted curve" developed with the same median but a standard deviation of β_{TOT} = 0.75. Even though the median collapse acceleration value is unchanged, as depicted in the figures, the additional uncertainty increases the collapse probability of the 3-storey hybrid building.

EVALUATION OF THE PROPOSED BASE SHEAR MODIFICATION FACTORS

FEMA P695 (2009) provides acceptability criteria to verify the adequacy of initially assumed force reduction factors based on the accepted collapse probabilities and total uncertainty. The acceptable values of adjusted collapse margin ratios are ACMR10% and ACMR20%, which correspond to 10% and 20% probability of collapse, respectively. The assumed R_d factor is acceptable if the calculated ACMR values within the performance group and individually exceed ACMR10% and ACMR20%, respectively. The ACMR10% and ACMR20% requirements corresponding to β_{TOT} = 0.75 are 2.61 and 1.88, respectively. Table 4 summarizes the performance evaluation process. The S_{MT} values in the table are obtained from the 2% in 50 years uniform hazard spectrum of Vancouver at the theoretical fundamental period of the hybrid buildings. For design base shear calculations, FEMA P695 (2009) suggests the use of the theoretical fundamental period over the periods from modal analysis. Tesfamariam et al. (2015) used the analytical period values for S_{MT} calculations and obtained conservative collapse risk for the same hybrid buildings. As summarized in the table, for all considered archetype buildings, the calculated individual and average ACMR values within the considered performance group exceed the FEMA P695 (2009) acceptability requirements. FEMA P695 (2009) recommends the largest overstrength value from all considered index archetypes as a system overstrength factor (R_o). From the static pushover analysis, the highest overstrength factor is 3.54. However, from a pragmatic perspective, the NBC 2010 (NRC 2010) limits the largest overstrength factor as 1.7. Based on this upper bound cutoff limit, for CLT infilled SMRFs, an overstrength factor of 1.5 is proposed.

DRIFT-EXCEEDANCE FRAGILITY CURVES

Seismic drift-exceedance fragility curves were developed from the IDA results corresponding to five EDP values: 1.5%, 2.5%, 5%, 7.5%, and collapse. The results are shown in Figure 11. These curves show the MISD exceedance probability when the structure is subjected to a given ground motion record. A fragility modeling algorithm developed by Baker (2014) was used to develop the CDFs by fitting a lognormal distribution of IMs at EDP of interest. The NBC 2010 (NRC 2010) and FEMA-356 (2000) represent an extensive damage (collapse prevention limit state) on SMRFs by MISD of 2.5% and 5%, respectively. For the 3-storey hybrid building, at S_{MT} = 0.72g, there is approximately 27.3% probability that the collapse prevention limit state of the NBC 2010 will be exceeded. Moreover, the probability of exceeding 5% MISD (collapse prevention limit state of the FEMA-356) is only 8%. Considering the drift exceedance fragility curves of the mid-rise hybrid building, as shown in Figure 11 (b), the probability of exceeding 2.5% MISD at S_{MT} = 0.5g, is 32.4%. The lowest exceedance probability is obtained for the 9-storey hybrid building; there is a 25.8% probability that the 2% in 50 years ground motion records will create an extensive damage on the building.

CONCLUSIONS

In this paper, seismic base shear modification factors were developed and validated using the collapse risk assessment approach of FEMA P695 for innovative timber-steel hybrid buildings. Archetype buildings of various heights were developed and designed according to the equivalent static load procedure of the NBC 2010. Nonlinear finite element models were developed using the OpenSees finite element package to perform nonlinear static and dynamic analyses. These models use experimentally calibrated connection material models and account for the frame-wall interaction using gap elements, which are implemented in a parallel fashion with the axial behaviour of the connections. Subsequently, a nonlinear static pushover analysis was performed to quantify the actual overstrength factors of the hybrid archetype buildings.

To check the FEMA P695 acceptable collapse probabilities, IDA was carried out using 60 ground motion records that are selected carefully to reflect regional seismicity in Vancouver, BC. Due to the complexity and the contributions of sub-crustal and subduction type earthquakes to the total seismic hazard, new ground motion selection criteria that considers all sources of earthquake for the given hazard, was developed. The adopted record selection method includes the effects of 'epsilon'. The data from IDA were then used to calculate the median collapse intensity and collapse margin ratio. Significant strain hardening was observed in the IDA responses. From IDA analysis results, to relate the scaled spectral acceleration values with the probability of collapse, collapse fragility curves were developed. Of all the analyzed buildings, the mid-rise hybrid building shows higher collapse safety.

The collapse safety and the exceedance probability of collapse prevention limit states were evaluated using ACMR values and seismic fragility curves, respectively. In general, for low and high-rise hybrid buildings, the probability of exceeding 2.5% MISD by the maximum considered earthquake, is less than 35%. From the static pushover analysis, the highest overstrength factor is 3.54. However, from the practicality perspective, the NBC 2010 limits the largest overstrength factor as 1.7. Based on this upper bound cutoff limit, for CLT infilled SMRFs, an overstrength factor of 1.5 is proposed. For all considered archetype buildings, the calculated individual and average ACMR values within the considered performance group exceeded the FEMA P695 acceptability requirements. From this research, it can be concluded that $R_o = 1.5$ and $R_d = 4$ will yield a safe and economical design of the proposed hybrid structure. The proposed values, however, should further be validated with experimental tests.

ACKNOWLEDGEMENTS

Funding for this research was provided by the British Columbia Forestry Innovation Investment's (FII) Wood First Program and the Natural Science Engineering Research Council of Canada Discovery Grant (RGPIN-2014-05013).

REFERENCES

ASCE. (2006). "Seismic rehabilitation of existing buildings." ASCE 41-06, Reston, VA.

ASTM E 2126 (2009). “Standard Test Methods for Cyclic (Reversed) Load Test for Shear Resistance of Vertical Elements of the Lateral Load Resisting Systems for Buildings.” ASTM International, West Conshohocken, PA, USA.

Atkinson, G.M. and Goda, K. (2011). Effects of seismicity models and new ground motion prediction equations on seismic hazard assessment for four Canadian cities. *Bulletin of the Seismological Society of America*, 101, 176-189.

Bezabeh, M. (2014). “Lateral behaviour and direct displacement based design of a novel hybrid structure: Cross laminated timber infilled steel moment resisting frames.” M.A.Sc. thesis, School of Engineering, Univ. of British Columbia, Canada.

Bezabeh, M., Tesfamariam, S., Stiemer, S., Popovski, M., Karacabeyli, E. (2015). “Direct displacement based design of a novel hybrid structure: steel moment-resisting frames with cross laminated timber infill walls.” *Earthquake Spectra*, in-press.

Ceccotti, A., Sandhaas, C., Okabe, M., Yasumura, M., Minowa, C., and Kawai, N. (2013). “SOFIE project—3D shaking table test on a seven storey full-scale cross-laminated building.” *Earthquake Eng. Struct. Dyn.*, 42(13), 2003–2021.

Dickof, C. (2013). “CLT infill panels in steel moment resisting frames as a hybrid seismic force resisting system.” M.A.Sc. thesis, Univ. of British Columbia, Canada.

Dickof, C., Stiemer, S., Bezabeh, M., and Tesfamariam, S. (2014). "CLT–steel hybrid system: ductility and overstrength values based on static pushover analysis." *J. Perform. Constr. Facil.*, 10.1061/(ASCE)CF.1943-5509.0000614, A4014012.

FEMA P695. 2009. Quantification of Building Seismic Performance Factors. Redwood City, California: Applied Technology Council.

Flatscher, G., Bratulic, K., & Schickhofer, G. (2014). “Screwed joints in cross laminated timber structures.” In Proceedings of the 13th World Conference on Timber Engineering, WCTE (2014), August 10-14, Quebec City, Canada.

Fragiacomo, M., Dujic, B., & Sustersic, I. (2011). “Elastic and ductile design of multi-storey crosslam massive wooden buildings under seismic actions.” *Engineering structures*, 33(11), 3043-3053.

Fragiacomo, M. and van de Lindt, J. (2016). "Special Issue on Seismic Resistant Timber Structures." J. Struct. Eng., 10.1061/(ASCE)ST.1943-541X.0001509, E2016001.

Gagnon, S., and Pirvu, C. (2011). Cross Laminated Timber Handbook, FPInnovations, Vancouver, Canada.

Goda, K. and Atkinson, G.M. (2011). Seismic performance of wood-frame houses in south-western British Columbia. *Earthquake Eng. Struct. Dyn.,*, 40, 903-924.

Goda, K. and Taylor, C.A. (2012). Effects of aftershocks on peak ductility demand due to strong ground motion records from shallow crustal earthquakes. *Earthquake Eng. Struct. Dyn.,*, 41, 2311-2330.

Goda, K., Wenzel, F., and De Risi, R. (2015). Empirical assessment of nonlinear seismic demand of mainshock-aftershock ground motion sequences for Japanese earthquakes. *Frontiers in Built Environment*, 1(6), doi: 10.3389/fbuil.2015.00006.

Hervé Poh'sié, G., Chisari, C., Rinaldin, G., Fragiacomo, M., Amadio, C., and Ceccotti, A. (2015). "Application of a translational tuned mass damper designed by means of genetic algorithms on a multistory cross-laminated timber building." *J. Struct. Eng.*, 10.1061/(ASCE)ST.1943-541X.0001342, E4015008.

Lignos, D. G., and Krawinkler, H. (2010). "Deterioration modeling of steel components in support of collapse prediction of steel moment frames under earthquake loading." *J. Struct. Eng.*, 10.1061/(ASCE)ST.1943 -541X.0000376, 1291–1302.

Mazzoni, S., McKenna, F., Scott, M., Fenves, G., and Jeremic, B. (2006). Open System for Earthquake Engineering Simulation, OpenSees, Berkeley, CA.

Mitchell, D., Tremblay, R., Karacabeyli, E., Paultre, P., Saatcioglu, M. and Anderson, D.L. (2003). "Seismic force modification factors for the proposed 2005 edition of the National Building Code of Canada." *Can. J. Civ. Eng.*, 30(2), 308-327.

NRCC (National Research Council of Canada). (2010). "National building code of Canada." Associate Committee on the National Building Code, Ottawa.

Pei, S., Popovski, M., and van de Lindt, J. W. (2013). “Analytical study on seismic force modification factors for cross-laminated timber buildings.” *Can. J. Civ. Eng.,* 40(9), 887–896.

Pei, S., van de Lindt, J., Popovski, M., Berman, J., Dolan, J., Ricles, J., Sause, R., Blomgren, H., and Rammer, D. (2014). "Cross-laminated timber for seismic regions: Progress and challenges for research and implementation." *J. Struct. Eng.*, 10.1061/(ASCE)ST.1943-541X.0001192, E2514001.

Popovski, M. and Gavric, I. (2015). "Performance of a 2-Story CLT House Subjected to Lateral Loads." *J. Struct. Eng.*, 10.1061/(ASCE)ST.1943-541X.0001315, E4015006.

Popovski, M., Schneider, J., and Schweinsteiger, M. (2010). “Lateral load resistance of cross-laminated wood panels.” Proc., 11th World Conf. on Timber Engineering (WCTE 2010), Riva del Garda, Italy.

Pozza, L., and Scotta, R. (2014). “Influence of wall assembly on behaviour of cross-laminated timber buildings.” *Proceedings of the ICE-Structures and Buildings*, 168(4), 275-286.

Rinaldin, G., Amadio, C., and Fragiacomo, M. (2013). “A component approach for the hysteretic behaviour of connections in cross-laminated wooden structures.” *Earthquake Eng. Struct. Dyn.*, 42(13), 2023–2042.

Schneider, J., Karacabeyli, E., Popovski, M., Stiemer, S., and Tesfamariam, S. (2014). “Damage assessment of connections used in cross-laminated timber subject to cyclic loads.” *J. Perform. Constr. Facil.*, 28, A4014008.

Shen, Y. L., Schneider, J., Tesfamariam, S., Stiemer, S. F., and Mu, Z. G. (2013). “Hysteresis behavior of bracket connection in cross-laminated timber shear walls.” *Constr. Build. Mater.*, 48, 980–991.

Stiemer, F., Dickof, C., and Tesfamariam, S. (2012a). “Timber-steel hybrid systems: Seismic overstrength and ductility factors.” Proc., 10th Int. Conf. on Advances in Steel Concrete Composite and Hybrid Structures, National Univ. of Singapore, Singapore, 2–4.

Stiemer, S., Tesfamariam, S., Karacabeyli, E., and Propovski, M. (2012b). “Development of steel-wood hybrid systems for buildings under dynamic loads.” STESSA 2012, Behaviour of Steel Structures in Seismic Areas. Santiago, Chile, January 9–11.

Tesfamariam, S., Stiemer, S. F., Dickof, C., and Bezabeh, M. A. (2014). “Seismic vulnerability assessment of hybrid steel-timber structure: Steel moment resisting frames with CLT infill.” *J. Earthquake Eng.*, 18(6), 929–944

Tesfamariam, S., Stiemer, S. F., Bezabeh, M., Goertz, C., Popovski, M., and Goda, K. (2015). “Force based design guideline for timber-steel hybrid structures : steel moment resisting frames with CLT infill walls.” doi:http://dx.doi.org/10.14288/1.0223405.

Vamvatsikos, D. and Cornell, C.A. (2002). “Incremental dynamic analysis.” *Earthquake Eng. Struct. Dyn.*, 31, 491-514. doi: 10.1002/eqe.141.

Yasumura, M., Kobayashi, K., Okabe, M., Miyake, T., and Matsumoto, K. (2015). "Full-scale tests and numerical analysis of low-rise CLT structures under lateral loading." *J. Struct. Eng.*, 10.1061/(ASCE)ST.1943-541X.0001348, E4015007.

Zhang, X., Fairhurst, M., and Tannert, T. (2015). "Ductility estimation for a novel timber–steel hybrid system." *J. Struct. Eng.*, 10.1061/(ASCE)ST.1943-541X.0001296, E4015001.

List of Figures

497

List of Tables

Table 1: Designed beam dimensions

Building storey	Storey no	External	Internal
3	1,2,3	W310×60	W310×45
6	1,2,3,4	W310×86	W310×79
	5,6	W310×74	W310×67
9	1,2,3,4	W310×107	W310×107
	5,6,7	W310×86	W310×86
	8,9	W310×79	W310×79

543

Table 2: Designed column dimensions

Building storey	Storey no	Left External	Right External	Internal
3	1	W310×67	W310×67	W310×67
	2, 3	W310×60	W310×60	W310×60
6	1,2,3,4	W310×129	W310×129	W310×129
	5,6	W310×86	W310×86	W310×86
9	1,2,3	W310×143	W310×143	W310×143
	4,5	W310×143	W310×143	W310×143
	7,8	W310×129	W310×129	W310×129
	9	W310×129	W310×129	W310×129

Table 3. CLT material properties

Material Property	Major Strength Direction	Minor Strength Direction
Elastic modulus, E_0 and E_{90} (MPa)	9500	9500
Compression strength, f_{c0} and f_{c90} (MPa)	11.5	11.5
Shear strength, f_{v0}, f_{v90} (MPa)	1.5	1.5
Bending at extreme fiber, f_{bo}, f_{b90} (MPa)	11.8	11.8
Tensile strength, f_{t0} and f_{t90} (MPa)	5.5	5.5

Table 4. Performance evaluation table

Performance group	**Hybrid Building Configuration**		**Calculated R_o and $ACMR$**				**Evaluation**	
	No. of storey	Infilled bays	R_o	S_{CT} (g)	S_{MT} (g)	$ACMR$	FEMA P695 requirement	Pass/fail
Low-rise	3	1	3.54	3.05	0.72	4.24	1.88	Pass
Average			**3.54**			**4.24**	**2.61**	Pass
Mid-rise	6	1	2.82	3.49	0.50	6.98	1.88	Pass
Average			**2.82**			**6.98**	**2.61**	Pass
High-rise	9	1	2.46	2.96	0.38	7.78	1.88	Pass
Average			**2.46**			**7.78**	**2.61**	Pass

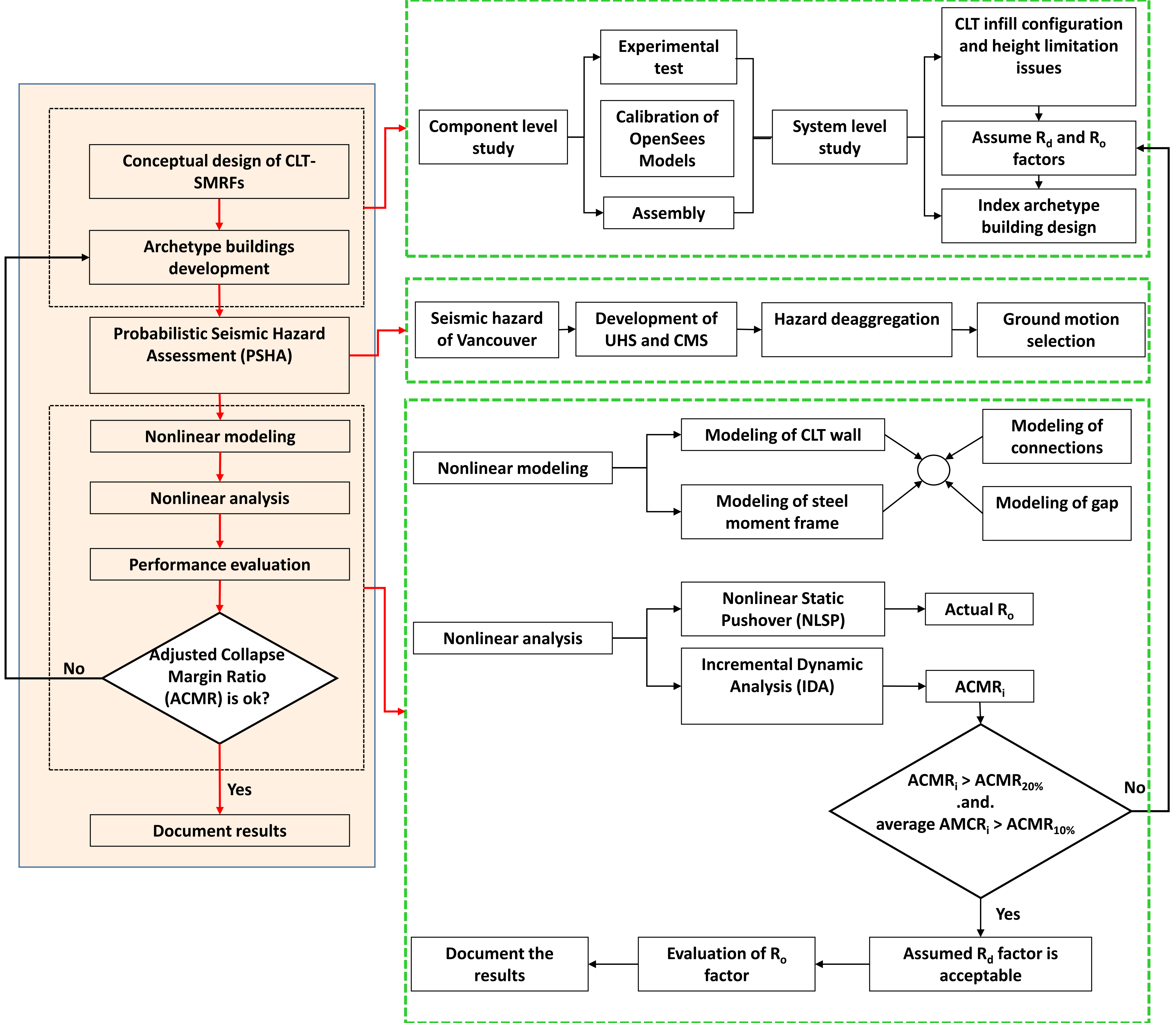

Conceptual design of CLT-SMRFs
Archetype buildings development
Probabilistic Seismic Hazard Assessment (PSHA)
Nonlinear modeling
Nonlinear analysis
Performance evaluation
Adjusted Collapse Margin Ratio (ACMR) is ok?
No
Yes
Document results
Component level study
Experimental test
Calibration of OpenSees Models
Assembly
System level study
CLT infill configuration and height limitation issues
Assume R_d and R_o factors
Index archetype building design
Seismic hazard of Vancouver
Development of UHS and CMS
Hazard deaggregation
Ground motion selection
Nonlinear modeling
Modeling of CLT wall
Modeling of steel moment frame
Modeling of connections
Modeling of gap
Nonlinear analysis
Nonlinear Static Pushover (NLSP)
Actual R_o
Incremental Dynamic Analysis (IDA)
$ACMR_i$
$ACMR_i > ACMR_{20\%}$
.and.
average $AMCR_i > ACMR_{10\%}$
No
Yes
Assumed R_d factor is acceptable
Evaluation of R_o factor
Document the results

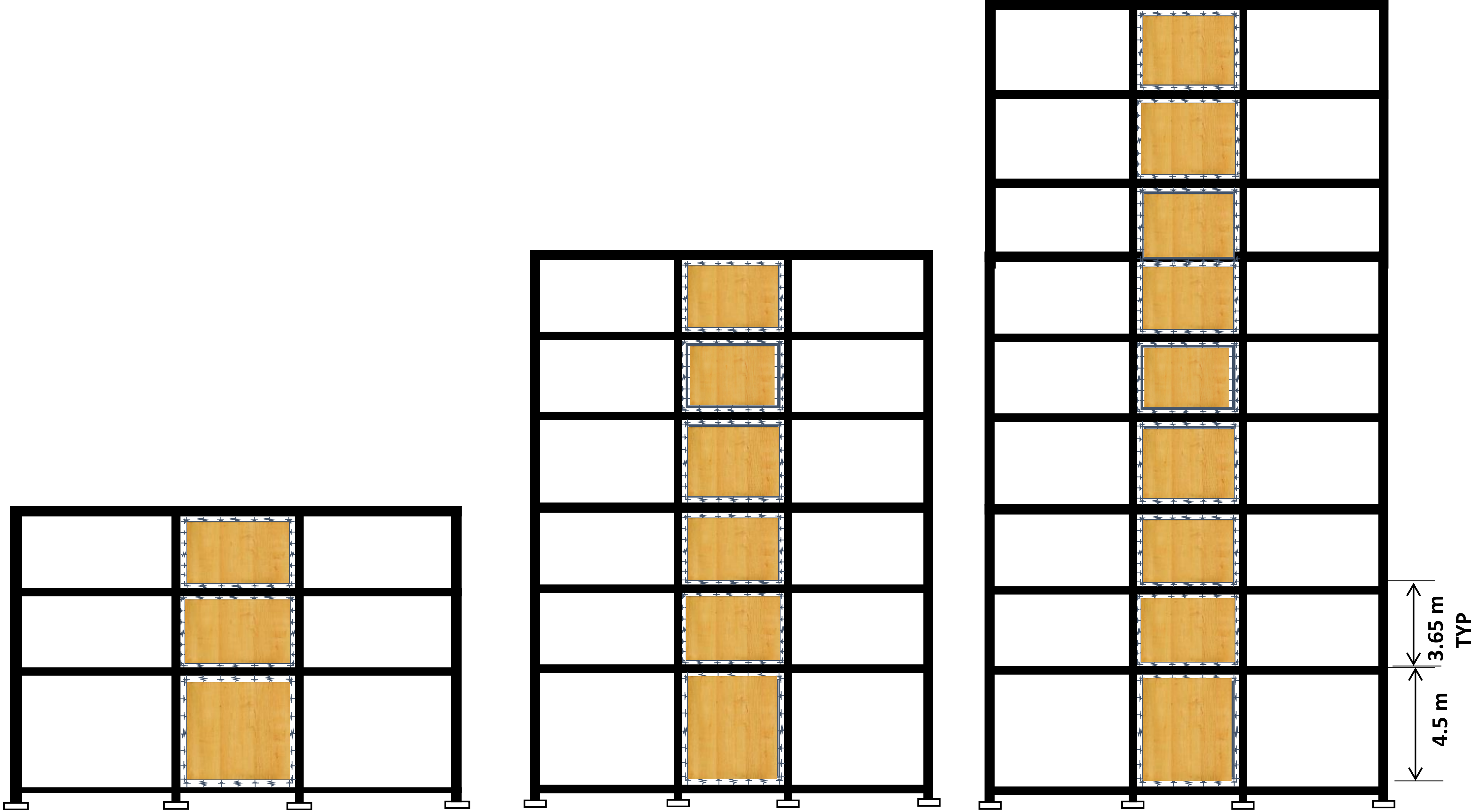

a) b) c)

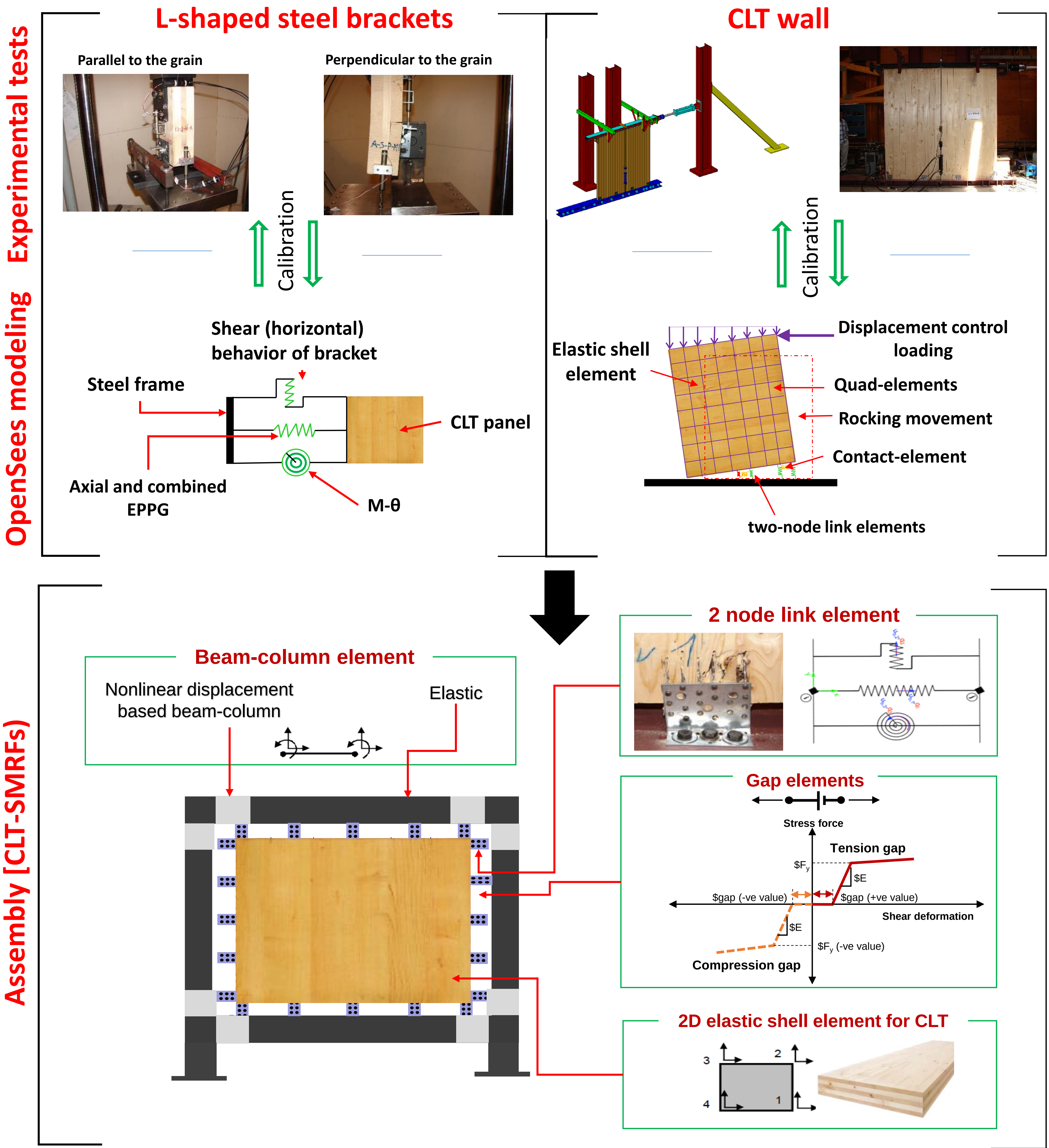

Experimental tests
OpenSees modeling
L-shaped steel brackets
Parallel to the grain
Perpendicular to the grain
Calibration
Shear (horizontal) behavior of bracket
Steel frame
CLT panel
Axial and combined EPPG
M-θ
CLT wall
Calibration
Elastic shell element
Displacement control loading
Quad-elements
Rocking movement
Contact-element
two-node link elements
Assembly [CLT-SMRFs)
Beam-column element
Nonlinear displacement based beam-column
Elastic
2 node link element
Gap elements
Stress force
Tension gap
F_y$
$E
$gap (-ve value)
$gap (+ve value)
Shear deformation
F_y$ (-ve value)
Compression gap
2D elastic shell element for CLT
3
2
4
1

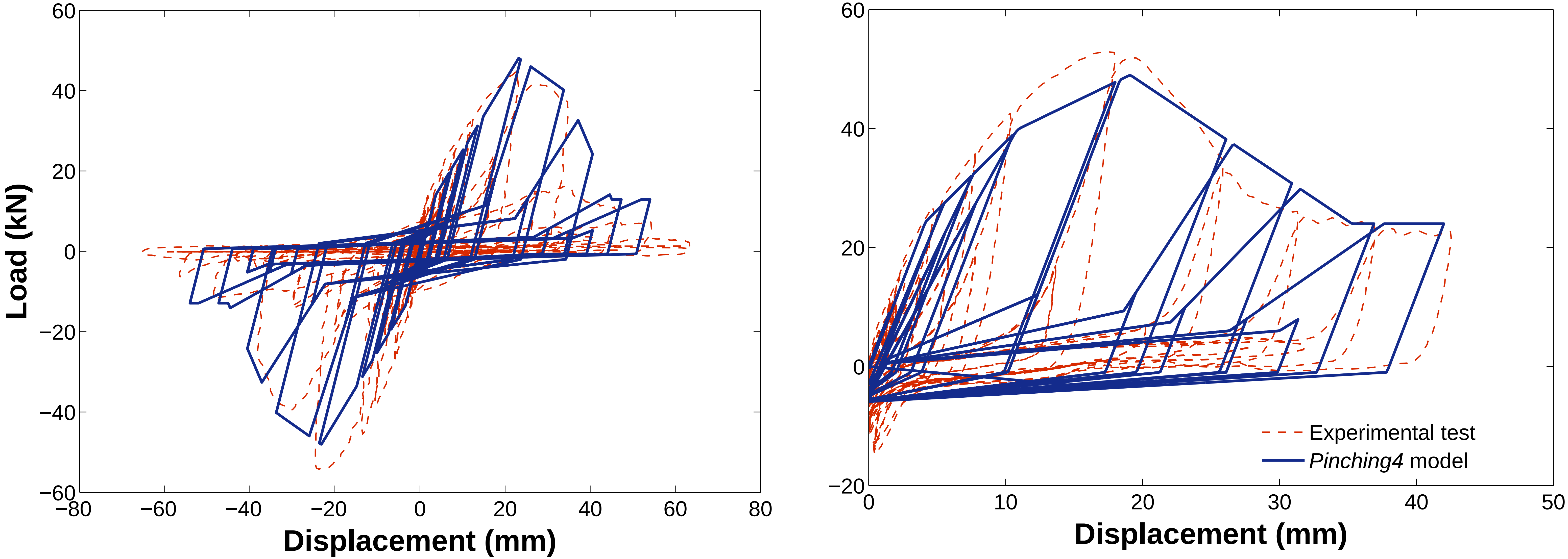

Load (kN)
Displacement (mm)
60
40
20
0
−20
−40
−60
−80
−60
−40
−20
0
20
40
60
80
Displacement (mm)
60
40
20
0
−20
0
10
20
30
40
50
Experimental test
Pinching4 model

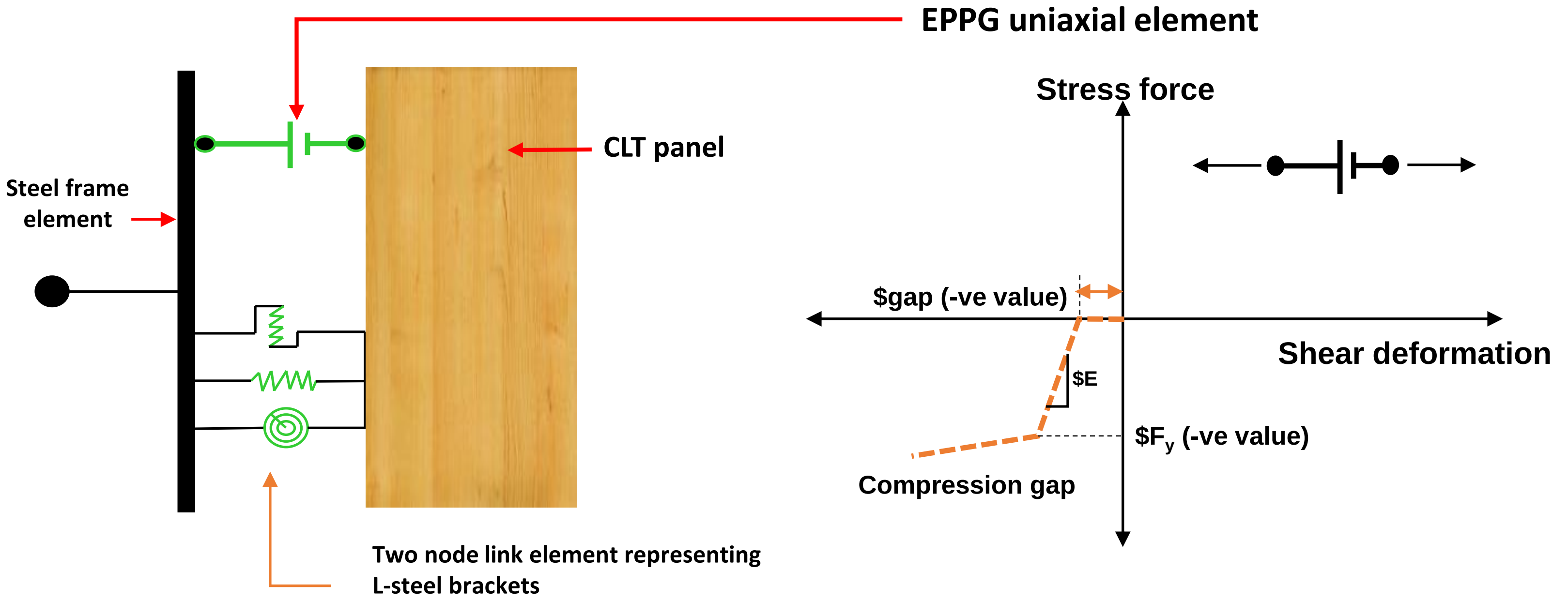
EPPG uniaxial element
Stress force
CLT panel
Steel frame element
$gap (-ve value)
Shear deformation
$E
F_y$ (-ve value)
Compression gap
Two node link element representing L-steel brackets

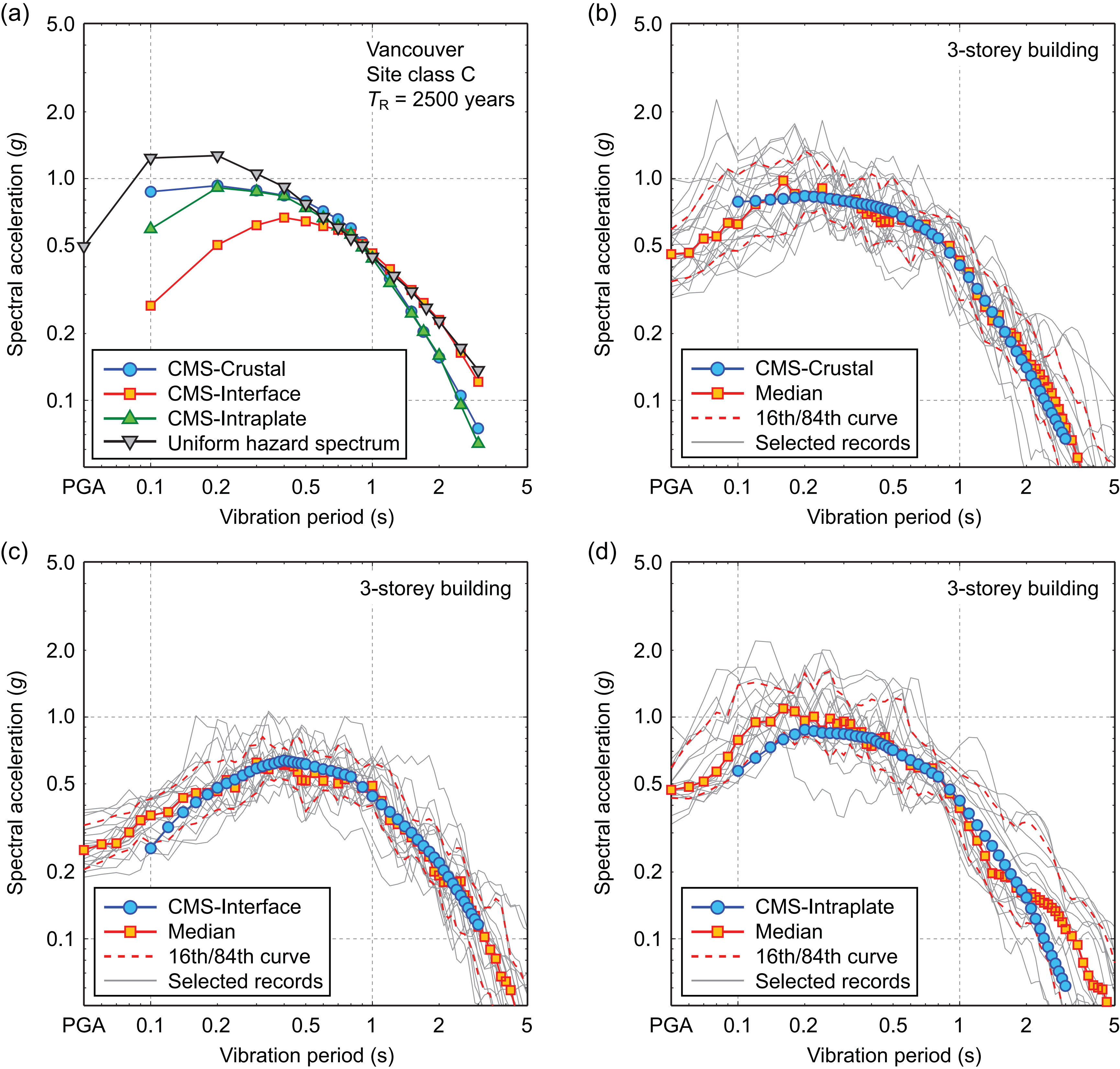

(a)
Vancouver
Site class C
T_R = 2500 years
CMS-Crustal
CMS-Interface
CMS-Intraplate
Uniform hazard spectrum
(b)
3-storey building
CMS-Crustal
Median
16th/84th curve
Selected records
(c)
3-storey building
CMS-Interface
Median
16th/84th curve
Selected records
(d)
3-storey building
CMS-Intraplate
Median
16th/84th curve
Selected records
Spectral acceleration (g)
Vibration period (s)
5.0
2.0
1.0
0.5
0.2
0.1
PGA
0.1
0.2
0.5
1
2
5

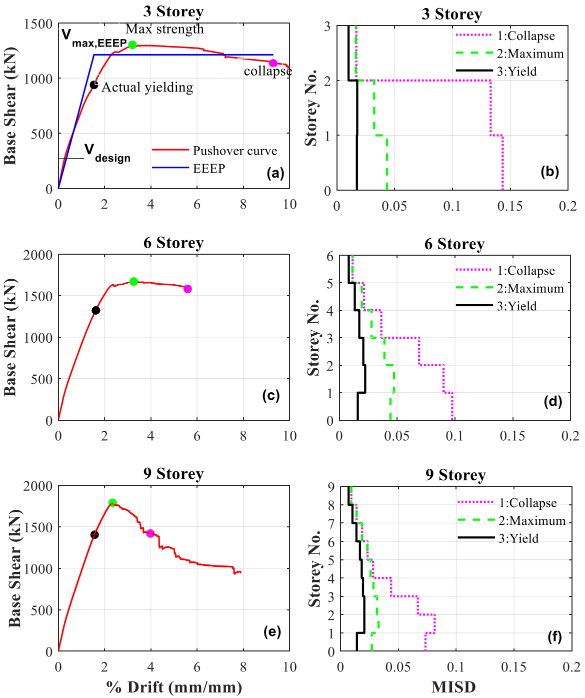

3 Storey
Base Shear (kN)
V max,EEEP
Max strength
collapse
Actual yielding
V design
Pushover curve
EEEP
(a)
Storey No.
1:Collapse
2:Maximum
3:Yield
(b)
6 Storey
(c)
(d)
9 Storey
(e)
(f)
% Drift (mm/mm)
MISD

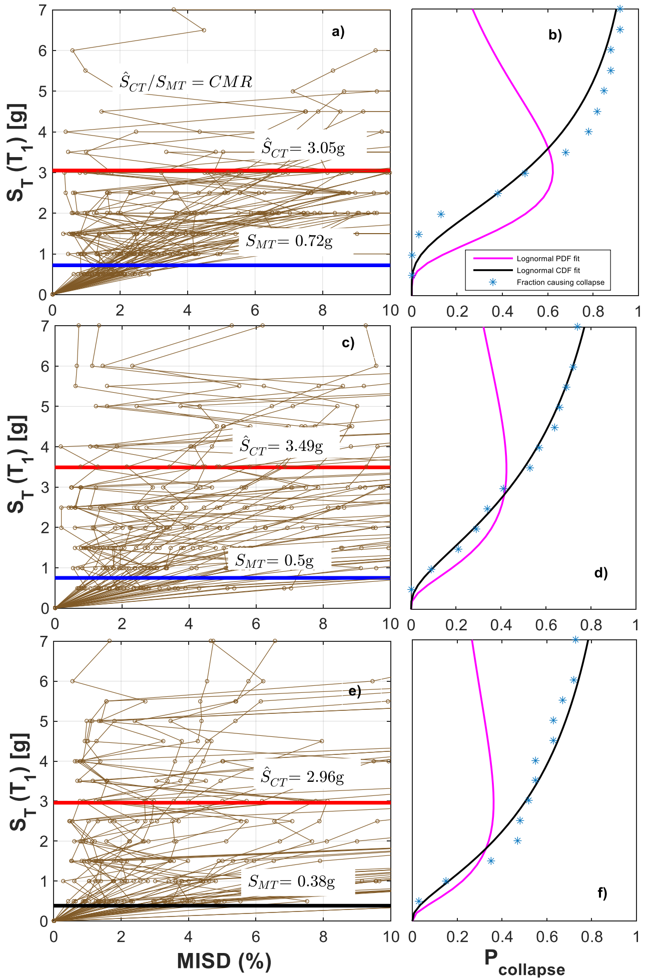

a)
b)
c)
d)
e)
f)
$\hat{S}_{CT}/S_{MT} = CMR$
$\hat{S}_{CT}$= 3.05g
S_{MT}= 0.72g
$\hat{S}_{CT}$= 3.49g
S_{MT}= 0.5g
$\hat{S}_{CT}$= 2.96g
S_{MT}= 0.38g
$S_T(T_1)$ [g]
MISD (%)
$P_{collapse}$
Lognormal PDF fit
Lognormal CDF fit
Fraction causing collapse

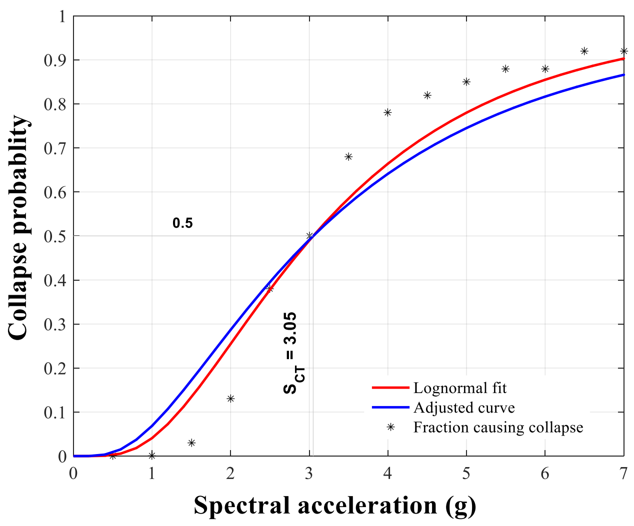
Collapse probablity
Spectral acceleration (g)
0.5
S_{CT} = 3.05
Lognormal fit
Adjusted curve
Fraction causing collapse
0
0.1
0.2
0.3
0.4
0.5
0.6
0.7
0.8
0.9
1
0
1
2
3
4
5
6
7

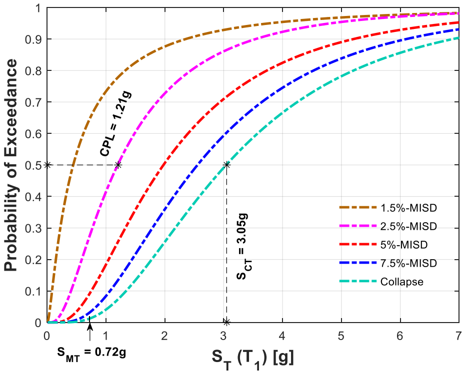

Probability of Exceedance
S_T (T_1) [g]
CPL = 1.21g
S_{CT} = 3.05g
S_{MT} = 0.72g
1.5%-MISD
2.5%-MISD
5%-MISD
7.5%-MISD
Collapse
0
0.1
0.2
0.3
0.4
0.5
0.6
0.7
0.8
0.9
1
0
1
2
3
4
5
6
7

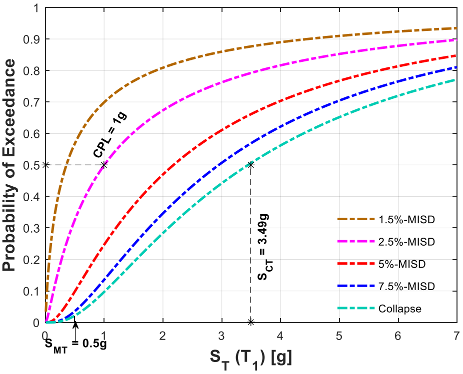

Probability of Exceedance
S_T (T_1) [g]
CPL = 1g
S_{CT} = 3.49g
S_{MT} = 0.5g
1.5%-MISD
2.5%-MISD
5%-MISD
7.5%-MISD
Collapse
0
0.1
0.2
0.3
0.4
0.5
0.6
0.7
0.8
0.9
1
0
1
2
3
4
5
6
7

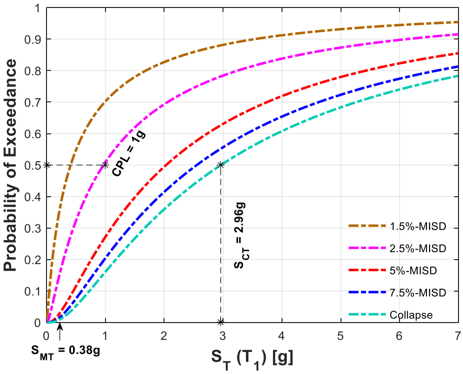

Probability of Exceedance
S_T (T_1) [g]
CPL = 1g
S_{CT} = 2.96g
S_{MT} = 0.38g
1.5%-MISD
2.5%-MISD
5%-MISD
7.5%-MISD
Collapse
0
0.1
0.2
0.3
0.4
0.5
0.6
0.7
0.8
0.9
1
0
1
2
3
4
5
6
7